Original Article
doi: 10.5115/acb.2011.44.2.106
pISSN 2093-3665 eISSN 2093-3673
Anatomy & Cell Biology acb

Immunohistochemical study on the expression of calcium binding proteins (calbindin-D28k, calretinin, and parvalbumin) in the cerebral cortex and in the hippocampal region of nNOS knock-out(–/–) mice

Yu Jin Cho[1], Jae Chul Lee[1], Bong Gu Kang[1,2], Jaeyeol An[1], Hyeon Suk Song[1,2], Onju Son[1], Do-Hyun Nam[2], Choong Ik Cha[1], Kyeung Min Joo[1]

[1]Department of Anatomy, College of Medicine, Seoul National University, [2]Department of Neurosurgery, School of Medicine, Sungkyunkwan University, Seoul, Korea

Abstract: Nitric oxide (NO) modulates the activities of various channels and receptors to participate in the regulation of neuronal intracellular Ca^{2+} levels. Ca^{2+} binding protein (CaBP) expression may also be altered by NO. Accordingly, we examined expression changes in calbindin-D28k, calretinin, and parvalbumin in the cerebral cortex and hippocampal region of neuronal NO synthase knockout(–/–) ($nNOS^{-/-}$) mice using immunohistochemistry. For the first time, we demonstrate that the expression of CaBPs is specifically altered in the cerebral cortex and hippocampal region of $nNOS^{-/-}$ mice and that their expression changed according to neuronal type. As changes in CaBP expression can influence temporal and spatial intracellular Ca^{2+} levels, it appears that NO may be involved in various functions, such as modulating neuronal Ca^{2+} homeostasis, regulating synaptic transmission, and neuroprotection, by influencing the expression of CaBPs. Therefore, these results suggest another mechanism by which NO participates in the regulation of neuronal Ca^{2+} homeostasis. However, the exact mechanisms of this regulation and its functional significance require further investigation.

Key words: Calcium binding proteins, Cerebral cortex and hippocampal region, Immunohistochemistry, Neuronal nitric oxide synthase (nNOS), nNOS knock-out(–/–) mice

Received March 24, 2011; Revised May 6, 2011; Accepted May 24, 2011

Introduction

Nitric oxide (NO) is synthesized from the amino acid L-arginine by the family of nitric oxide synthase (NOS) enzymes [1]. Neuronal NOS (nNOS) is a major isoform that produces NO in the brain [2]. Regulation of NO synthesis is mainly mediated by cytosolic Ca^{2+} levels. Ca^{2+} influx from extracellular fluid and the release of Ca^{2+} from intracellular stores increases Ca^{2+} concentrations in the neuronal cytoplasm. Ca^{2+} binds calmodulin (CaM) and the Ca^{2+}-CaM complex activates nNOS by direct binding. Ca^{2+} released

Corresponding author:
Kyeung Min Joo and Choong Ik Cha
Department of Anatomy, College of Medicine, Seoul National University, 28 Yeongeon-dong, Jongno-gu, Seoul 110-799, Korea
Kyeung Min Joo: Tel: +82-2-740-8204, Fax: +82-2-745-9528, E-mail: kmjoo@snu.ac.kr
Choong Ik Cha: Tel: +82-2-740-8205, Fax: +82-2-745-9528, E-mail: cicha@snu.ac.kr
*Yu Jin Cho and Jae Chul Lee have contributed equally to this work.

from intracellular Ca^{2+} stores is also modulated by NO. NO induces ryanodine receptor phosphorylation through protein kinase G, which results in increased Ca^{2+} release from the endoplasmic reticulum into the cytoplasm [3-5]. The entire neuronal Ca^{2+} homeostasis regulatory system consists of a Ca^{2+} entry system, intracellular Ca^{2+} stores, a Ca^{2+} extrusion system, and a Ca^{2+} buffer. It is hypothesized that NO participates in the regulation of Ca^{2+} homeostasis through mechanisms other than by modulating the Ca^{2+} entry system and intracellular Ca^{2+} stores.

Calcium binding proteins (CaBPs) are thought to play a major role in buffering intracellular Ca^{2+} and to be involved in a variety of Ca^{2+}-mediated signal transduction events [6-8]. Three CaBPs, namely calbindin-D28k (CB), parvalbumin (PV), and calretinin (CR), which are members of the EF-hand calcium-binding protein family, have been implicated to play a neuroprotective role in various pathological conditions by functioning as buffers for excess calcium. CaBPs such as CB [9, 10] and CR [11] colocalize with nNOS in some neuron populations. Similar cerebellar functional defects are detected in both nNOS [12] and CaBP knockout mice [13, 14]. Based on these findings, Ca^{2+} buffering may be a candidate for Ca^{2+} homeostatic regulation by NO.

We have carefully examined CaBP expressional changes in nNOS knock-out(−/−) ($nNOS^{-/-}$) mice immunohistochemically [15] to support the possibility that NO regulates the neuronal Ca^{2+} buffering system by modulating CaBP expression and that this regulation differs according to neuronal type. CB, CR, and PV are highly expressed in the cerebral cortex and hippocampal region [16-18], Our study shows, for the first time, that the expression of CB, CR, and PV changes specifically in the cerebral cortex and hippocampal region of $nNOS^{-/-}$ mice.

Materials and Methods

Ten male $nNOS^{-/-}$ B6, 129S4-$Nos1^{tm1Plh}$/J (3-4 months old) mice and 12 male control B6129SF2/J (3-4 months old) mice were examined using immunohistochemistry. The B6129SF2/J mice are F2 hybrids with a mixed C57BL/6× 129 background (designated B6;129) and suggested to be used as approximate physiological controls for the $nNOS^{-/-}$ B6, 129S4-$Nos1^{tm1Plh}$/J mice by the Jackson Laboratory (Bar Harbor, ME, USA). The $nNOS^{-/-}$ mice were obtained from Dr. Oh (Induced Mutant Resources Program, Genetic Resources Center, Korea Research Institute of Bioscience and Biotechnology, Daejeon, Korea). All animals were bred under specific pathogen-free conditions and maintained under standard laboratory conditions on a 12 hour light/dark cycle with free access to food and water. The experiments were conducted in accordance with the National Institutes of Health (NIH) Guide for the Care and Use of Laboratory Animals (NIH publication no. 80-23, revised 1996). The animals were perfused transcardially with cold 0.05 M phosphate buffered saline (pH 7.4) and then with ice-cold 4% paraformaldehyde. Brains were cryoprotected in a series of cold sucrose solutions and were cut at 40 μm in the coronal plane. Immunohistochemistry was performed using the free-floating method described previously [19]. Rabbit anti-CB polyclonal antibody, rabbit anti-CR polyclonal antibody, and anti-PV monoclonal antibody (AB1778 and AB5054, respectively, Chemicon International, Temecula, CA, USA; and P3088 for PV, Sigma, St. Louis, MO, USA) were used as primary antibodies.

Some sections was reacted without primary antiserum, and different samples were exposed to primary antiserum that had been preabsorbed for 24 hours with control antigen peptides. Sections from these samples did not exhibit any immunoreactivity. We randomly selected five unit areas in the cerebrum of control (n=12) and $nNOS^{-/-}$ mice (n=10) and calculated the numbers of CB, CR, and PV-immunoreactive neurons per unit area. Sections from each control and $nNOS^{-/-}$ group were stained together to eliminate conflicts between experimental conditions. Visual assessment and densitometric measurements using the Scion Image program (NIH, Bethesda, MD, USA) was used to determine staining density. Student's *t*-test was performed to investigate whether changes in CaBP expression were statistically significant ($^{*}P<0.01$).

Immunohistochemistry images were taken using a ProgRes C14 digital camera with ProgRes C14 software (JENOPTIC Laser, Optic, System, Munich, Germany). Image editing software (Adobe Photoshop) was used to adjust the size and contrast and to combine the images.

Results

Numerous CB-immunoreactive neurons were observed in the cerebral cortex of control mice (Fig. 1A), which were divided into two categories; neurons expressing high levels

doi: 10.5115/acb.2011.44.2.106

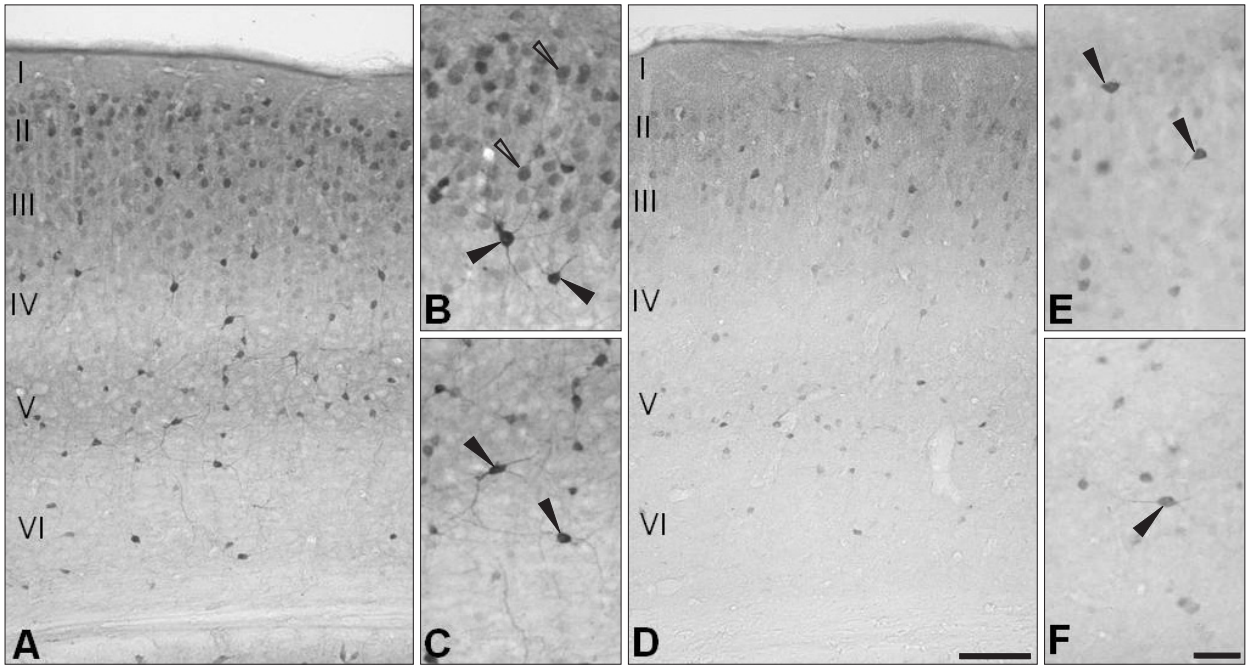

Fig. 1. Changes in calbindin D28k (CB) immunoreactivity in the cerebral cortex of neuronal NO synthase knockout(−/−) (nNOS$^{-/-}$) mice (D-F) compared with control mice (A-C). (B, E) are high power views of layers II and III and (C, F) are high power views of layer V of the cerebral cortex. The distribution pattern and morphology of CB-immunoreactive neurons were similar in the control and nNOS$^{-/-}$ mice (A, D). CB immunoreactivity in nNOS$^{-/-}$ mice was much lower than that of control mice (D-F) and the high power views show that lengths of the CB-immunoreactive neurites in the nNOS$^{-/-}$ mice were shorter and less branched than those of the control mice (black arrowheads in E and F). Scale bars=200 μm (A, D), 50 μm (B, C, E, F).

of CB in their neurites and cell bodies (black arrowheads in Fig. 1B, C), and those expressing CB only in their cell bodies (white arrowheads in Fig. 1B). The former neurons were distributed in all layers of the cerebral cortex except layer I (Fig. 1A) and had long CB-immunoreactive neurites that branched many times (black arrowheads in Fig. 1B, C). The former seemed to express more CB than the latter (Fig. 1B). The latter type of neurons were localized in layers II and III and they outnumbered the former (Fig. 1A). These two kinds of CB-immunoreactive neurons were also observed in nNOS$^{-/-}$ mice, and their morphology and distribution pattern were similar (Fig. 1D, E). However, the number of neurons expressing high CB levels in their cell bodies and neurites was reduced significantly in nNOS$^{-/-}$ mice (Table 1, Fig. 1D) and each individual neuron of this type showed lower levels of CB immunoreactivity than that in control mice (Fig. 1E, F). On high power, the lengths of CB-immunoreactive neurites were also reduced in nNOS$^{-/-}$ mice and they had fewer branches (black arrowheads in Fig. 1E, F). As for the former type neurons, the number of neurons expressing CB only in the cell bodies and their CB immunoreactivity was reduced in nNOS$^{-/-}$ mice (Fig. 1E). Because it was difficult to

Table 1. Changes of the numbers of calbindin-D28k, calretinin, and parvalbumin-immunoreactive neurons in the cerebral cortex and in the hippocampal region of nNOS$^{-/-}$ mice

Area	Control (12 animals)	Knock-out (10 animals)
Calbindin-D28k		
Cerebral cortex[a]	149.4±18.2	93.8±14.3*
Hippocampal region		
CA1[b]	18.1±5.2	9.2±3.1*
CA3[b]	5.3±1.8	4.0±2.8
Calretinin		
Cerebral cortex	121.3±14.1	88.0±18.2*
Hippocampal region		
CA1	20.4±5.3	14.2±1.9*
CA3	5.7±4.0	2.8±1.9
Dentate gyrus[c]	5.6±1.7	2.9±1.1*
Parvalbumin		
Cerebral cortex	286.1±42.2	282.5±49.3
Hippocampal region		
CA1	51.3±7.4	49.6±12.1
CA3	29.2±9.8	23.7±5.4
Dentate gyrus	8.4±3.9	12.0±4.7

Values are the mean±standard deviations. Student's *t*-test was performed (*P<0.05). nNOS$^{-/-}$, neuronal NO synthase knockout(−/−); CB, calbindin-D28k; CR, calretinin. [a]Only neurons expressing high levels of CB in their cell bodies and neurites were included. [b]Only CB-immunoreactive neurons other than pyramidal cells were included. [c]Only CR-immunoreactive neurons in the polymorph layer of the dentate gyrus were included.

Table 2. Changes of calbindin-D28k, calretinin, and parvalbumin-immunoreactivity in the cerebral cortex and in the hippocampal region of nNOS$^{-/-}$ mice

Area	Control (12 animals)	Knock-out (10 animals)
Calbindin-D28k		
Cerebral cortex		
Layer II-III	89.1±16.9	66.2±21.2*
Hippocampal region		
Anterior part		
CA1 (pyramidal layer)	93.1±4.8	43.0±1.9*
CA3 (stratum lucidum)	112.4 ± 4.2	71.8±2.4*
Dentate gyrus (granule cell layer)	117.9±3.4	83.2±7.6*
Posterior part		
CA2 (pyramidal layer)	87.6±3.6	50.2±4.2*
Calretinin		
Hippocampal region		
Dentate gyrus (subgranular zone)	150.6±4.3	109.7±2.0*

Mean density is the sum of the gray values of all the pixels in the selection that was divided by the number of pixels within the selection. Values are the mean±standard deviations. Student's *t*-test was performed (*P<0.05). nNOS$^{-/-}$, neuronal NO synthase knockout(−/−).

determine the individual neurons of this type due to overlap, a densitometric analysis was performed using Scion Image to determine the significance of these changes. As a result, the decrease in CB immunoreactivity observed in layers II and III was statistically significant (Table 2).

The hippocampal region of control mice showed a highly specific CB expression pattern (Fig. 2A). Granule cells in the dentate gyrus expressed high levels of CB in their cell bodies, and relatively high CB immunoreactivity was observed in the neuropil of the molecular layer and in the polymorph layer (Fig. 2A, C, I). In Ammon's horn of the anterior hippocampal region, cell bodies of pyramidal cells in CA1 showed CB immunoreactivity, but those of pyramidal cells in CA3 did not (Fig. 2A, D, E). Instead, the neuropil of the stratum lucidum in CA3 expressed high levels of CB (Fig. 2A, E). In contrast to the anterior hippocampal region, pyramidal cells in CA1-2 of the posterior hippocampal region expressed CB not only in their cell bodies but also in their neurites, which were oriented to the stratum radiatum (Fig. 2I, J). Additionally, several neurons in CA1 and CA3, other than pyramidal cells, expressed high levels of CB (Fig. 2A, black arrowheads in Fig. 2D, E). These neurons expressed CB in their neurites as well as their cell bodies, and their cell bodies were located in all layers of Ammon's horn. As observed in the cerebral cortex, neurons and neuropil expressing CB in the hippocampal region of control mice showed the same CB expression pattern in the hippocampal region of nNOS$^{-/-}$ mice. However, the CB expression levels of these neurons and neuropil was lower in the nNOS$^{-/-}$ mice than that in control mice (Fig. 2B, F-H, K, L). The number of CB-immunoreactive neurons other than pyramidal cells in CA1 was significantly lower and each neuron showed less CB immunoreactivity in nNOS$^{-/-}$ mice than that in controls (Table 1, Fig. 2B, F-H). Also, there tended to be fewer neurons of this type in CA3, although this result was not statistically significant (Table 1, Fig. 2B). Because it was difficult to identify individual CB-immunoreactive granule cells in the dentate gyrus and CB-immunoreactive pyramidal cells in CA1-2 due to overlap, and cell number could not be used in the analysis of CB-immunoreactive neuropil in the stratum lucidum of CA3, densitometric analysis using Scion Image was performed to determine whether reductions in CB immunoreactivity were statistically significant. According to this analysis, the CB-immunoreactive changes in granule cells, pyramidal cells, and the neuropil were statistically significant (Table 2).

CR-immunoreactive neurons were present in more superficial layers of the cerebral cortex of control mice (Fig. 3A), and CR was expressed in the cell bodies and neurites (Fig. 3A-C). Several types of neurons expressed CR. For example, some CR-immunoreactive neurons had bipolar neuron morphology (Fig. 3B), whereas others had multipolar neuron morphology (Fig. 3C). Although the cerebral cortex of nNOS$^{-/-}$ mice had a similar CR expression pattern, the level of CR immunoreactivity was much lower than that of the controls (Fig. 3D-F). The nNOS$^{-/-}$ mice had a significantly lower number of CR-immunoreactive neurons (Table 1, Fig. 3D) and each CR-immunoreactive neuron showed lower levels of CR immunoreactivity. Additionally, the CR-immunoreactive neurites of the nNOS$^{-/-}$ mice tended to decrease in number, but this change was not statistically significant (Fig. 3E, F).

In control mice, a high level of CR was prominently expressed in the neuropil of the subgranular zone of the dentate gyrus, whereas the cell bodies of granule cells showed no CR immunoreactivity (Fig. 3G, I). In the polymorph layer of the dentate gyrus several CR-immunoreactive neurons were observed near the granule cell layer, and this CR immunoreactivity was confined to the cell bodies (Fig. 3G, I). In CA1 and CA3 of Ammon's horn, pyramidal cells showed slight CR immunoreactivity which could not be distinguished from background signals (Fig. 3G, J, K). Several neurons highly expressing CR, which were not pyramidal cells, were widely distributed in CA1 and CA3 (Fig. 3G). Their cell bodies were located in all layers of Ammon's horn,

doi: 10.5115/acb.2011.44.2.106

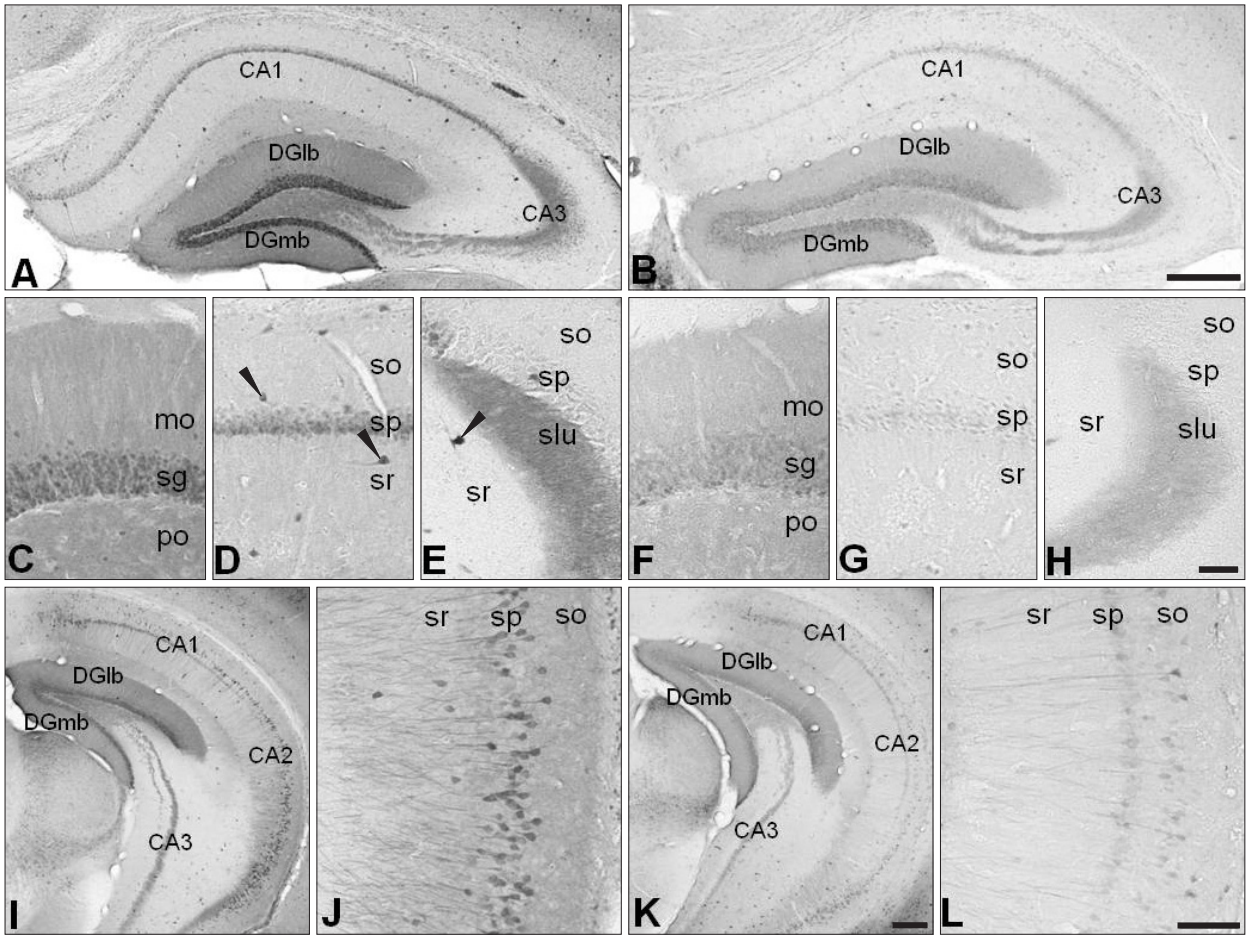

Fig. 2. Decreased calbindin D28k (CB) expression in the hippocampal region of neuronal NO synthase knockout(−/−) (nNOS$^{-/-}$) mice (A, C-E, I, J for the control mice and B, F-H, K, L for the nNOS$^{-/-}$ mice). (C and F, D and G, and E and H) are high power views of the dentate gyrus, CA1 of Ammon's horn, and CA3 of Ammon's horn, respectively. The overall distribution patterns of CB-immunoreactivity and the morphology of CB-immunoreactive neurons were similar in the control and nNOS$^{-/-}$ mice (A-L). CB immunoreactivity was much reduced in the neuronal cell bodies and the neuropil of nNOS$^{-/-}$ mice (B, F-H, K, L). CA1, field CA1 Ammon's horn; CA2, field CA2 Ammon's horn; CA3, field CA3 Ammon's horn; DGlb, dentate gyrus lateral blade; DGmb, dentate gyrus medial blade; mo, molecular layer; sg, granule cell layer; po, polymorph layer; so, stratum oriens; sp, pyramidal layer; sr, stratum radiatum; slu, stratum lucidum. Scale bars=200 μm (A, B), 50 μm (C-H), 100 μm (I, K), 80 μm (J, L).

and they had long CR-immunoreactive neurites extending through Ammon's horn (Fig. 3G, J, K). No differences were observed between the anterior and posterior regions of the hippocampal region, and CA2 showed CR expression resembling that of CA1. The hippocampal region of the nNOS$^{-/-}$ mice had a CR expression pattern similar to that of control mice (Fig. 3H, L-N). However, overall CR immunoreactivity was markedly downregulated in nNOS$^{-/-}$ mice. CR immunoreactivity of the neuropil in the dentate gyrus was significantly lower in nNOS$^{-/-}$ mice than that in control mice (Table 2, Fig. 3H, L), as were the numbers of CR-immunoreactive neurons in CA1 and in the polymorph layer of the dentate gyrus (Table 1, Fig. 3H). Although it was not statistically significant, the number of CR-immunoreactive neurons in CA3 tended to be reduced (Table 1, Fig. 3H). In contrast to the cerebral cortex where the decrease in the number of CR-immunoreactive neurons was accompanied by a reduction in the lengths of CB-immunoreactive neurites, the lengths of the CB-immunoreactive neurites and CR-immunoreactive neurons in Ammon's horn of nNOS$^{-/-}$ mice were unchanged (Fig. 3M, N).

Many PV-immunoreactive neurons were observed in the cerebral cortex of control mice (Fig. 4A). In contrast to CR, they were concentrated in deeper layers of the cerebral cortex (Fig. 4A). These neurons had multipolar morphology, and PV was expressed in their cell bodies and neurites, which were shorter than those of CB-immunoreactive and CR-immunoreactive neurons (Fig. 4B). This PV expression

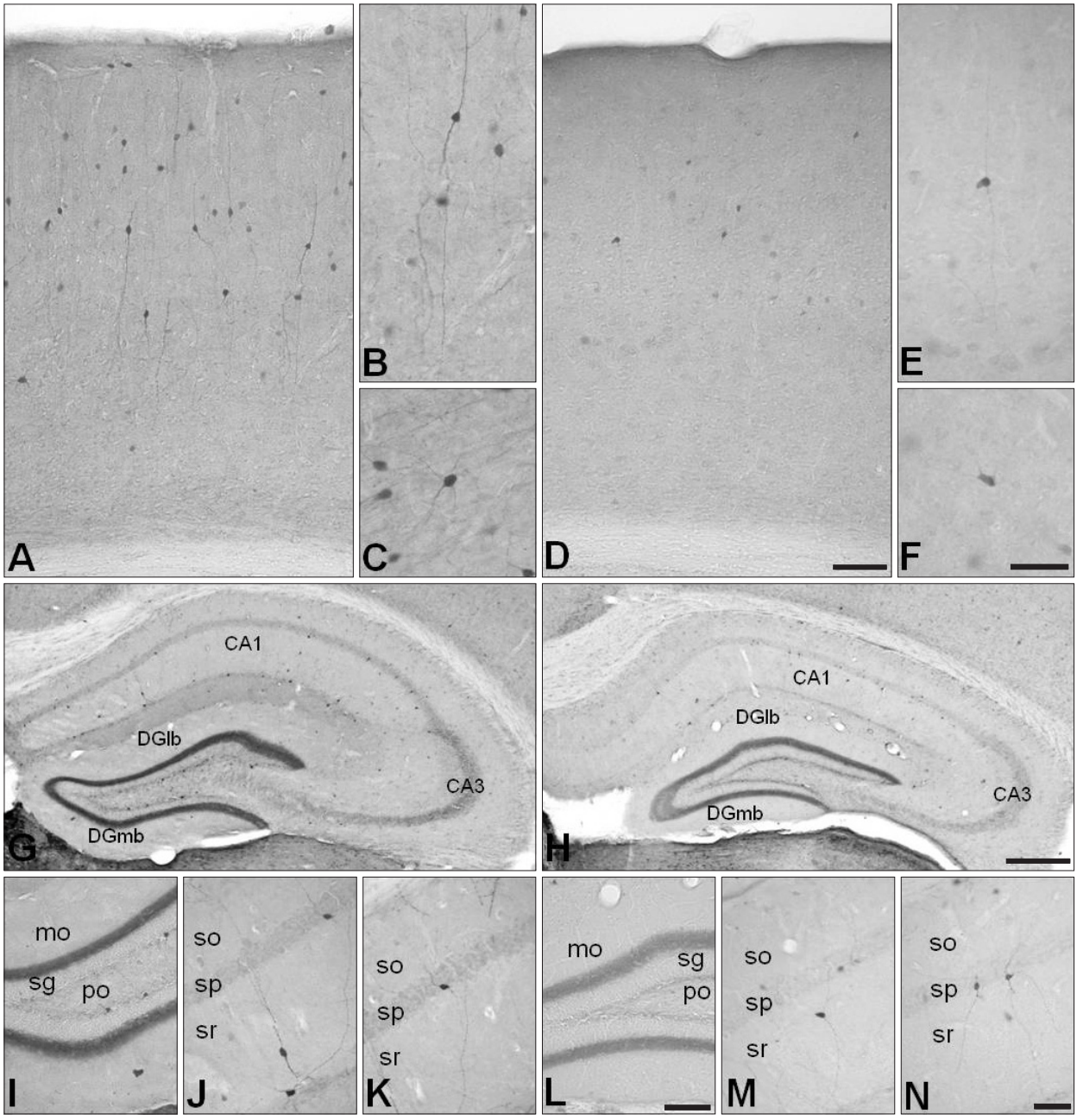

Fig. 3. Changes in calretinin (CR) immunoreactivity in the cerebral cortex (D-F) and in the hippocampal region (H, L-N) of neuronal NO synthase knockout(−/−) ($nNOS^{-/-}$) mice, compared with those of control mice (A-C for the cerebral cortex and G, I-K for the hippocampal region). (I and L, J and K, and M and N) are high power views of the dentate gyrus and the CA1 of Ammon's horn, respectively. In the cerebral cortex and hippocampal region, the overall distribution patterns of CR-immunoreactivity and the morphology of CR-immunoreactive neurons were similar in the control and $nNOS^{-/-}$ mice (A-N). In the cerebral cortex, $nNOS^{-/-}$ mice had fewer CR-immunoreactive neurons and each CR-immunoreactive neuron showed less CR-immunoreactivity than that in control mice (D-F). High power views showed that the lengths of the CR-immunoreactive neurites in the $nNOS^{-/-}$ mice were shorter than those of the control mice (D-F). Calbindin D28k (CB) immunoreactivity in the neuropil of the dentate gyrus was much reduced in the hippocampal region of $nNOS^{-/-}$ mice (H, L) and the number of CR-immunoreactive neurons was less (H) in $nNOS^{-/-}$ mice, although the morphology of these neurons was preserved (L-N). CA1, field CA1 Ammon's horn; CA3, field CA3 Ammon's horn; DGlb, dentate gyrus lateral blade; DGmb, dentate gyrus medial blade; mo, molecular layer; sg, granule cell layer; po, polymorph layer; so, stratum oriens; sp, pyramidal layer; sr, stratum radiatum. Scale bars=150 μm (A, D), 80 μm (B, C, E, F), 200 μm (G, H), 65 μm (I, L), 50 μm (J, K, M, N).

doi: 10.5115/acb.2011.44.2.106

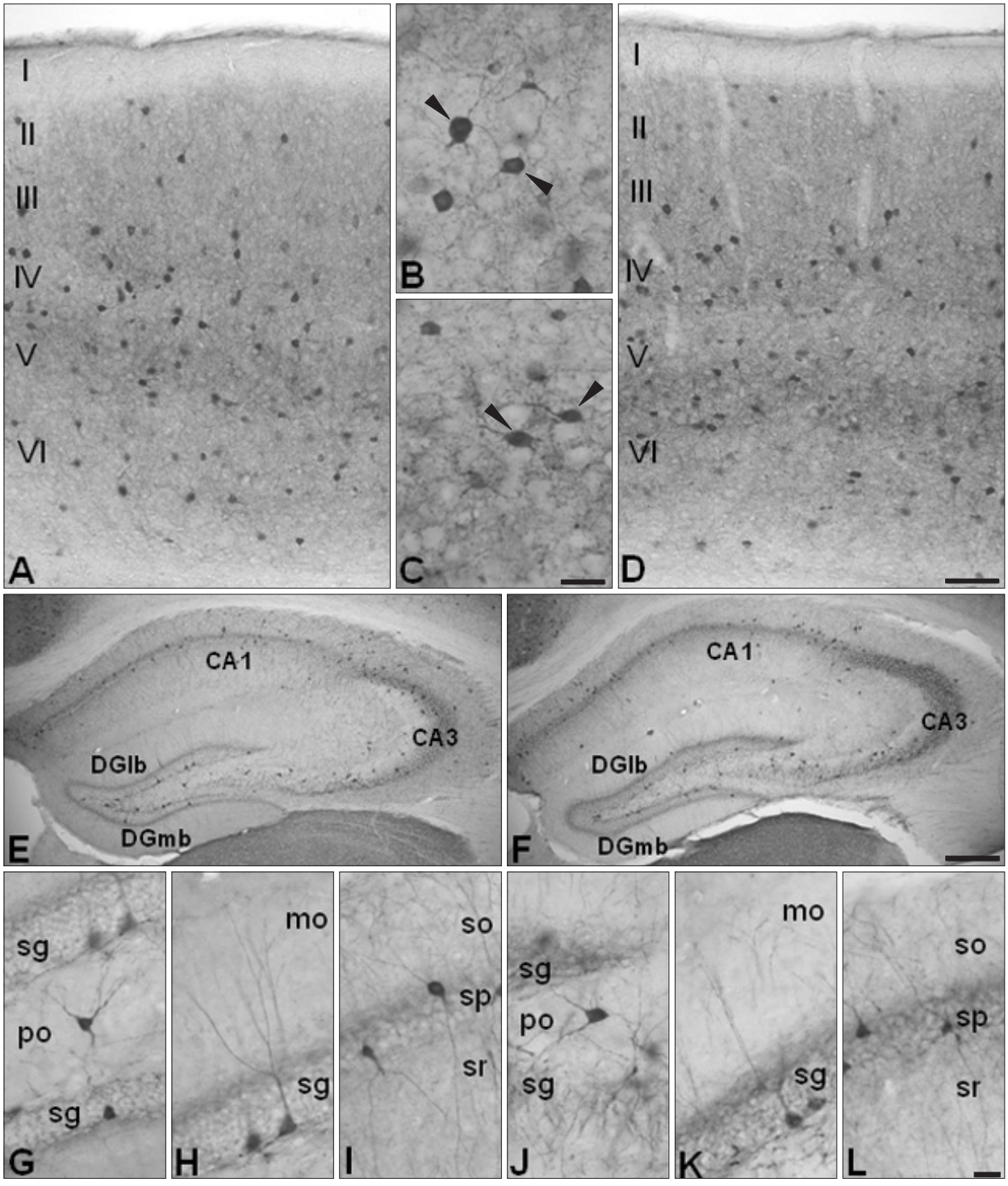

Fig. 4. Parvalbumin (PV) immunoreactivity in the cerebral cortex (A-D) and hippocampal region (E-L) of control mice (A, B, E, G-I) and neuronal NO synthase knockout(−/−) ($nNOS^{-/-}$) mice (C, D, F, J-L). (B and C, G and J, H and K, and I and L) are high power views of the cerebral cortex, the polymorph layer of the dentate gyrus, the granule cell layer of the dentate gyrus, and the pyramidal layer of Ammon's horn, respectively. The numbers of PV-immunoreactive neurons, their distribution patterns, and morphology were unchanged in the cerebral cortex and hippocampal region of $nNOS^{-/-}$ mice (F, J-L). CA1, field CA1 Ammon's horn; CA3, field CA3 Ammon's horn; DGlb, dentate gyrus lateral blade; DGmb, dentate gyrus medial blade; sg, granule cell layer; po, polymorph layer; mo, molecular layer;so, stratum oriens; sp, pyramidal layer; sr, stratum radiatum. Scale bars=150 μm (A, D), 60 μm (B, C), 200 μm (E, F), 40 μm (G-L).

pattern was preserved in most regions of the cerebral cortex (Fig. 4C, D). Additionally, a cell count analysis showed that the number of PV-immunoreactive neurons was unchanged in the cerebral cortex of nNOS$^{-/-}$ mice (Table 1). Granule cells in the dentate gyrus and pyramidal cells in Ammon's horn did not express PV (Fig. 4E, G-I); however, the neuropil around the cell bodies of granule cells and pyramidal cells showed relatively high PV immunoreactivity. Many PV-immunoreactive neurons, other than granule cells and pyramidal cells, were observed in all regions of the hippocampal region and expressed PV in their cell bodies and neurites (Fig. 4E, G-I). These neurons were concentrated in the granule cell layer of the dentate gyrus and in the pyramidal layer of Ammon's horn or near these layers (Fig. 4E). These PV expression patterns were well preserved in nNOS$^{-/-}$ mice (Fig. 4F, J-L). As observed in the cerebral cortex, the number of PV-immunoreactive neurons was unchanged in the hippocampus of nNOS$^{-/-}$ mice (Table 1), and the PV-immunoreactive neurons of nNOS$^{-/-}$ mice had morphologies that were similar to those of control mice (Fig. 4J-L).

Discussion

Using immunohistochemical techniques we found that CB and CR expression levels were characteristically altered in the cerebral cortex and hippocampal region of nNOS$^{-/-}$ mice (Figs. 1-3). We also found that different neuronal types in the cerebral cortex and hippocampal region showed different CB and CR expression in nNOS$^{-/-}$ mice. In contrast, PV expression in the cerebral cortex and hippocampal region of nNOS$^{-/-}$ mice showed few differences when compared to control mice (Fig. 4). As the number of neurons in the central nervous system is not significantly altered in nNOS$^{-/-}$ mice [15], these changes in CB and CR expression may be due to their changing expression rather than to altered numbers of CB-immunoreactive and CR-immunoreactive neurons. Because CaBP expression patterns did not change in nNOS$^{-/-}$ mice, it seems that NO influenced only their expression levels and not their expression patterns. It is concluded that NO modulates CB and CR expression levels in the cerebral cortex and hippocampal region in a cell-type specific manner, and that NO may differentially affect Ca^{2+} homeostasis in many types of neurons.

Previously, the morphologies of neurons expressing CB, CR, and PV were examined in the cerebral cortex, and these CaBPs were expressed mainly by non-overlapping subpopulations of gamma aminobutyric acid (GABA)ergic neurons, although some CB-immunoreactive pyramidal cells were observed mainly in layer III [20]. Among these GABAergic interneurons, the most characteristic morphological type of GABAergic interneurons immunoreactive for CB were double bouquet cells; and they were bipolar, double bouquet, and Cajal-Retzius cells for CR; and double bouquet and large basket cells for PV. As each CaBP is expressed by different subpopulations of GABAergic neurons [20], these CaBPs are used to classify GABAergic interneurons in the cerebral cortex with other neuropeptides and physiological characteristics [18, 21]. In this classification, GABAergic interneurons are classified into four groups based on their chemical properties; PV cells, somatostatin cells (most also express CB), vasoactive intestinal peptide (VIP) cells (some express CR or cholecystokinin [CCK]), and large CCK cells.

In this study, we found that neuronal CB and CR expression was downregulated, whereas neuronal PV expression was unchanged in the cerebral cortex of nNOS$^{-/-}$ mice. As the morphological classification of GABAergic interneurons is based on their specific placement of synapses onto different target cell domains, it is difficult to precisely identify the GABAergic interneurons using only immunohistochemical results. However, as found in a previous study [20], some CB-immunoreactive neurons in layer V appeared to be double bouquet cells with fusiform cell bodies (Fig. 1C black arrowheads), and pyramidal-like cells in layers II and III showed weak CB immunoreactivity (Fig. 1B white arrowheads). In addition, CR-immunoreactive and PV-immunoreactive neurons had morphologies similar to those reported previously [20]; i.e., CR-immunoreactive neurons had a bipolar morphology (bipolar cells, Fig. 3B), CR-immunoreactive neurons near pia matter had horizontal axes (Cajal-Retzius cells, Fig. 3A), and PV-immunoreactive neurons had large cell bodies (large basket cells, Fig. 4B). Each antibody seemed to specifically detect neurons expressing its counterpart. Thus, it can be concluded that NO activated CB and CR expression in pyramidal cells, somatostatin cells, and VIP cells but did not affect PV expression in PV cells.

Various cell types in the hippocampal region express CaBPs [17, 22]. Among excitatory cells, granule cells of the dentate gyrus and pyramidal cells of CA1 expressed CB. Furthermore, mossy cells in the hilar region of the

doi: 10.5115/acb.2011.44.2.106

dentate gyrus were CR- and PV-immunoreactivity. The most characteristic morphological types of GABAergic interneurons immunoreactive for CB were bistratified cells and other interneurons innervating dendrites of pyramidal neurons, whereas those immunoreactive to CR were spiny and spine-free neurons; and those immunoreactive to PV were basket cells and chandelier cells. In addition to these cellular components, the neuropil of the hippocampal region also showed characteristic CaBP expression patterns; CB and CR are highly expressed in the neuropil of the stratum lucidum of CA3 [23] and in the neuropil of the subgranular zone of the dentate gyrus [24], respectively. As observed in the cerebral cortex, CaBP expression in GABAergic interneurons of the hippocampal region did not overlap [17]. Therefore, CaBPs are also used to classify GABAergic interneurons in this region, but their morphological, chemical, and physiological properties are too varied to allow their classification into several groups in contrast to the cerebral cortex [25].

Characteristic CaBP expression patterns in the hippocampal region were also observed in this study. As previously reported [17], CB is expressed by granule cells of the dentate gyrus, pyramidal cells of CA1, and the neuropil in the stratum lucidum of CA3 (Fig. 2). High CR immunoreactivity was observed in the neuropil of the subgranular zone of the dentate gyrus (Fig. 3), whereas principal neurons, except mossy cells of the dentate gyrus, showed little CR- or PV-immunoreactivity (Figs. 3, 4). Moreover, PV-immunoreactive interneurons were distributed near the pyramidal layer of Ammon's horn and the granule cell layer of the dentate gyrus and showed typical radial morphology (Fig. 4H, I), as previously reported [17]. Because we observed that CB and CR expression was reduced in the hippocampus of $nNOS^{-/-}$ mice, whereas PV immunoreactivity was unchanged, it can be concluded that NO modulates the Ca^{2+} buffering capacity of CA1 pyramidal cells, granule cells of the dentate gyrus, and subpopulations of hippocampal GABAergic interneurons (bistratified cells and other interneurons innervating dendrites of pyramidal neurons) by modulating their CB expression. NO further regulates Ca^{2+} buffering capacity of mossy cells in the dentate gyrus and subpopulations of hippocampal GABAergic interneurons (spiny and spine-free CR-immunoreactive neurons) by modulating their CR expression. In contrast, Ca^{2+} buffering capacity of basket cells and chandelier cells may not be regulated by NO.

For the first time, we demonstrated that CaBP expression, such as CB, CR, and PV, are specifically altered in the cerebral cortex and hippocampal region of $nNOS^{-/-}$ mice and that their expression changed based on neuronal type. These results suggest another mechanism by which NO participates in the regulation of neuronal Ca^{2+} homeostasis. However, the exact mechanisms of this regulation and their functional significance requires further investigation.

Acknowledgements

This work was supported by grant no. 09-2010-001 from the SNUH Research Fund.

References

1. Moncada S, Higgs A. The L-arginine-nitric oxide pathway. N Engl J Med 1993;329:2002-12.
2. Liu PK, Robertson CS, Valadka A. The association between neuronal nitric oxide synthase and neuronal sensitivity in the brain after brain injury. Ann N Y Acad Sci 2002;962:226-41.
3. Clementi E, Riccio M, Sciorati C, Nisticò G, Meldolesi J. The type 2 ryanodine receptor of neurosecretory PC12 cells is activated by cyclic ADP-ribose. Role of the nitric oxide/cGMP pathway. J Biol Chem 1996;271:17739-45.
4. Short DM, Heron ID, Birse-Archbold JL, Kerr LE, Sharkey J, McCulloch J. Apoptosis induced by staurosporine alters chaperone and endoplasmic reticulum proteins: identification by quantitative proteomics. Proteomics 2007;7:3085-96.
5. Mattson MP. Apoptosis in neurodegenerative disorders. Nat Rev Mol Cell Biol 2000;1:120-9.
6. Rogers JH. Calretinin: a gene for a novel calcium-binding protein expressed principally in neurons. J Cell Biol 1987;105:1343-53.
7. Polans A, Baehr W, Palczewski K. Turned on by Ca2+! The physiology and pathology of Ca(2+)-binding proteins in the retina. Trends Neurosci 1996;19:547-54.
8. Schäfer BW, Heizmann CW. The S100 family of EF-hand calcium-binding proteins: functions and pathology. Trends Biochem Sci 1996;21:134-40.
9. Geula C, Schatz CR, Mesulam MM. Differential localization of NADPH-diaphorase and calbindin-D28k within the cholinergic neurons of the basal forebrain, striatum and brainstem in the rat, monkey, baboon and human. Neuroscience 1993;54:461-76.
10. Bertini G, Peng ZC, Bentivoglio M. The chemical heterogeneity of cortical interneurons: nitric oxide synthase vs. calbindin and parvalbumin immunoreactivity in the rat. Brain Res Bull 1996;39:261-6.
11. Arévalo R, Sánchez F, Alonso JR, Rubio M, Aijón J, Vázquez R. Infrequent cellular coexistence of NADPH-diaphorase and calretinin in the neurosecretory nuclei and adjacent areas of the rat hypothalamus. J Chem Neuroanat 1993;6:335-41.

12. Nelson RJ, Demas GE, Huang PL, Fishman MC, Dawson VL, Dawson TM, Snyder SH. Behavioural abnormalities in male mice lacking neuronal nitric oxide synthase. Nature 1995;378:383-6.
13. Airaksinen MS, Eilers J, Garaschuk O, Thoenen H, Konnerth A, Meyer M. Ataxia and altered dendritic calcium signaling in mice carrying a targeted null mutation of the calbindin D28k gene. Proc Natl Acad Sci U S A 1997;94:1488-93.
14. Cheron G, Schurmans S, Lohof A, d'Alcantara P, Meyer M, Draye JP, Parmentier M, Schiffmann SN. Electrophysiological behavior of Purkinje cells and motor coordination in calretinin knock-out mice. Prog Brain Res 2000;124:299-308.
15. Huang PL, Dawson TM, Bredt DS, Snyder SH, Fishman MC. Targeted disruption of the neuronal nitric oxide synthase gene. Cell 1993;75:1273-86.
16. Baimbridge KG, Celio MR, Rogers JH. Calcium-binding proteins in the nervous system. Trends Neurosci 1992;15:303-8.
17. Freund TF, Buzsáki G. Interneurons of the hippocampus. Hippocampus 1996;6:347-470.
18. Kawaguchi Y, Kubota Y. GABAergic cell subtypes and their synaptic connections in rat frontal cortex. Cereb Cortex 1997;7:476-86.
19. Lee JC, Cho YJ, Kim J, Kim N, Kang BG, Cha CI, Joo KM. Region-specific changes in the immunoreactivity of vasoactive intestinal peptide and pituitary adenylate cyclase-activating polypeptide receptors (VPAC2, and PAC1 receptor) in the aged rat brains. Brain Res 2010;1351:32-40.
20. DeFelipe J. Types of neurons, synaptic connections and chemical characteristics of cells immunoreactive for calbindin-D28K, parvalbumin and calretinin in the neocortex. J Chem Neuroanat 1997;14:1-19.
21. Kawaguchi Y, Kondo S. Parvalbumin, somatostatin and cholecystokinin as chemical markers for specific GABAergic interneuron types in the rat frontal cortex. J Neurocytol 2002;31:277-87.
22. Jinno S, Kosaka T. Patterns of expression of calcium binding proteins and neuronal nitric oxide synthase in different populations of hippocampal GABAergic neurons in mice. J Comp Neurol 2002;449:1-25.
23. Jouvenceau A, Potier B, Battini R, Ferrari S, Dutar P, Billard JM. Glutamatergic synaptic responses and long-term potentiation are impaired in the CA1 hippocampal area of calbindin D(28k)-deficient mice. Synapse 1999;33:172-80.
24. Schurmans S, Schiffmann SN, Gurden H, Lemaire M, Lipp HP, Schwam V, Pochet R, Imperato A, Böhme GA, Parmentier M. Impaired long-term potentiation induction in dentate gyrus of calretinin-deficient mice. Proc Natl Acad Sci U S A 1997;94:10415-20.
25. Parra P, Gulyás AI, Miles R. How many subtypes of inhibitory cells in the hippocampus? Neuron 1998;20:983-93.